

DETECTION OF FLOODED AREAS FOLLOWING THE 2011 THAILAND FLOODS USING ASTER IMAGES

Jun SHIMAKAGE^{*a} and Fumio YAMAZAKI^b

^a Graduate Student, Department of Urban Environment Systems, Chiba University,
1-33, Yayoi-cho, Inage-ku, Chiba, 263-8522, Japan Tel: +81-43-290-3528
E-mail: j.shimakage@chiba-u.jp

^b Professor, Department of Urban Environment Systems, Chiba University,
1-33, Yayoi-cho, Inage-ku, Chiba, 263-8522, Japan Tel: +81-43-290-3557
E-mail: fumio.yamazaki@faculty.chiba-u.jp

KEY WORDS: 2011 Thailand flood, ASTER, NDVI, visible near-infrared bands, threshold value

Abstract: In the autumn of 2011, large-scale floods occurred in the central Thailand. A large amount of water flowed down to wide areas of Thailand and brought serious damages for a long period. Approximately 9% of the whole nation's area suffered from the floods. Many industrial estates were affected, and it caused the disruption of the supply chains of international industries. In this study, ASTER sensor was used to grasp this widespread disaster. False color composite, NDVI and surface temperature images were made from ASTER's VNIR and TIR bands obtained before and during the 2011 Thailand floods. The flooded areas were estimated by the decrease of the NDVI value and surface temperature in the daytime. Comparing the histograms of pre-flood and during-flood NDVI values, a threshold value of NDVI for water body was determined. As a result, the transition of flooded areas could be extracted properly from the ASTER VNIR images.

INTRODUCTION

In the autumn of 2011, large scale floods occurred in the central Thailand. A large amount of water flowed down to wide areas of Thailand. Many associated failures occurred in civil infrastructures and lifeline networks, and hence the floods brought serious effects for a long period. Approximately 9% of the whole nation's area in 44 prefectures out of 77 prefectures suffered from the floods. Many industrial estates were affected, and it caused the disruption of the supply chains of world's industries, such as automobile and electronics. The effects further influenced the world economy.

In order to grasp large-scale disasters at an early stage, the use of satellite remote sensing is effective due to its characteristics of broad-area coverage at one time and remotely, with a long period of archives. ASTER (Advanced Spaceborne Thermal Emission and Reflection Radiometer) onboard Terra satellite with 15-m resolution in visible near-infrared (VNIR) bands, 30-m resolution short-wavelength infrared (SWIR) bands, and 90-m resolution thermal-infrared (TIR) bands has been used to grasp widespread disasters in the world since 1999. The use of ASTER images thus has a great advantage to grasp large-scale disaster such as the 2011 floods in Thailand.

For the 2004 Indian Ocean tsunami caused by the Sumatra earthquake, Kouchi and Yamazaki (2007) extracted the inundated areas by tsunami in Khaolak, southern Thailand, using pre- and post-event ASTER's VNIR and SWIR images. The reduction of the Normalized Difference Vegetation Index (NDVI) was clearly observed in the areas where vegetation became dead or reduced due to salt water, and a such situation was confirmed in the field survey (Yamazaki *et al.*, 2005). For grasping flooded areas due to the collapse of embankments of Asuwa River, occurred in the 2004 Fukui heavy rainfall in Japan, Kato (2007) used a false color composite and NDVI from ASTER images. He demonstrated the usefulness of these images to detect flooded areas, especially by a remarkable reduction of NDVI on the flooded ground surface. For the 2011 Tohoku earthquake, Hanada and Yamazaki (2012) estimated flooded areas by tsunami using the surface temperature distributions from pre- and post-event ASTER TIR images, both at daytime and nighttime. The estimated results were compared with the change of corresponding NDVI values and a map from aerial survey and they were found to be in good agreement.

For the 2011 central Thailand floods, International Charter -Space and major Disaster (2011) was activated due to the request from Asia Disaster Reduction Center (ADRC) on 17 October 2011. Dr. Masahiko Nagai of Asian Institute of Technology (AIT) was assigned as the project manager and his team engaged in analysing various optical and SAR satellite images provided from space agencies and companies in the world. However, AIT campus, located in the northern Bangkok, was also inundated by the flood on 21 October 2011 and thus the team evacuated from their campus but they continued the analysis of the satellite data at their temporary evacuation site (Asian Institute of Technology, 2011). In this flood event, Japan Aerospace Exploration Agency (JAXA) conducted aerial

survey of the flooded areas by Pi-SAR-L, the same L-band SAR system to be onboard ALOS-2 in 2013, from 5 to 27 November 2011 in collaboration with Geo-Informatics and Space Technology Development Agency (GISTDA) of Thailand (JAXA, 2011).

Field surveys of the floods were carried out by several international teams. Komori (2011) reported the observation in their field survey and illustrated the precipitation, flow capacity and flood situation in the Chao Phraya River basin, including the flood fighting activities in industrial estates and central Bangkok. Field surveys were also carried out by a team of Japanese and Thai researchers (Yamazaki, 2011) to collect ground truth data of satellite images during (November 5 to 7, 2011) and after (February 6 and 7, 2012) the flood. The GPS synchronized ground photographs were taken in the surveys and they were compared with satellite images in this paper.

In this study, ASTER's VNIR and TIR images acquired before and during the 2011 Thailand floods were used to access the situation in the affected areas. False color composite, NDVI, and surface temperature images were produced from ASTER data before and during the floods. The flooded areas were estimated from the decrease of NDVI value and the decrease of surface temperature in the daytime. In addition, from the comparison of pre-event and during-event NDVI's histograms, a threshold value for the NDVI corresponding to water body was assumed. The transition of the flooded areas was evaluated by applying the threshold to multi-temporal ASTER images.

FIELD SURVEY PHOTOS AND ASTER IMAGES USED IN THIS STUDY

The study area of this paper was selected as a part of Chao Phraya River basin, about 30 km in width and 100 km in length from the north of Ayutthaya to the Gulf of Thailand through the capital city Bangkok, as shown in Figure 1 (a). This region is the heart of Indochina as well as the most important one for the Kingdom of Thailand since it contains the center of administration and economy (Bangkok), cultural heritage (Ayutthaya), international and domestic air transportation hubs (Suvarnabhumi and Don Mueang Airports) and also a number of industrial parks operated by Industrial Estate Authority of Thailand.

The ground photos with GPS data obtained in the field survey on November 5 to 7, 2011 were shown in Figure 1, where (c) to (f) were taken in Nava Nakorn Industrial Estate and (g) to (i) in the central Bangkok.

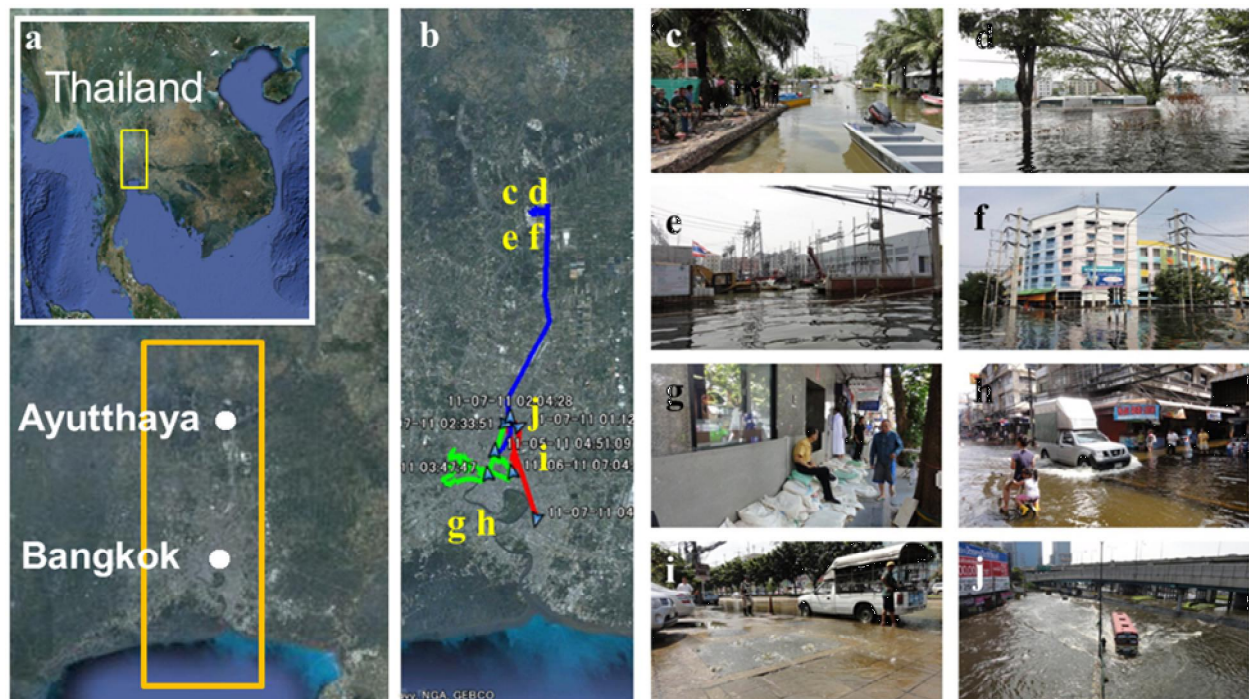


Figure 1: (a) Location of the study area, (b) Field survey routes on November 5 (blue), November 6 (green), and November 7 (red), 2011 and photo shooting points, (c) Survey on a boat in Nava Nakorn Industrial Estate, (d) Buses almost completely under water (e) A factory with its ground floor completely submerged, (f) Flooded road recognized only by utility poles and trees, (g) Sandbags and temporary concrete walls installed around buildings in the central Bangkok, (h) A flooded area in the west bank of Chao Phraya River, where daily life was still going on, (i) Water coming out from the cover plate of underground drainage ducts on sidewalk, (j) Flooded main street where only buses and trucks were going through in the water.

The satellite images obtained from ASTER sensor onboard NASA's Terra satellite were used to access the flooded area by the 2011 central Thailand floods. ASTER is a high-performance optical sensor developed by the Ministry of International Trade and Industry (MITI, currently METI) of Japan. It has 3 bands in Visible and Near-Infrared (VNIR) radiometer with 15 m resolution, 6 bands in Short-Wavelength Infrared (SWIR) radiometer with 30 m resolution (currently out of order), and 5 bands in Thermal-Infrared (TIR) radiometer with 90 m resolution, 14 observation channels in total. Out of these channels, band 10 in TIR, bands 1 (G), 2 (R), and 3 (NIR) in VNIR were used in this study.

As a pre-event image before the floods, one observed on December 13, 2009 was used. As VNIR images during the floods, those observed on October 23 and 25, and November 1, 8, 10 and 17, 2011 were employed to detect the flood situation of the study area. TIR images were also acquired on December 13, 2009, and November 1 and 17, 2011 and those images were also used to access the capability of TIR in flood monitoring. Both the VNIR and TIR images were observed from 3:48 to 4:10 in the local time of Thailand, or from 10:48 to 11:10 in GMT. Note that the images on October 23 and 25 were combined as one image with less clouds since they included many cloud-covered areas. The images on November 8 and 10 were also combined to obtain the same observed area with the others. By these image combinations, we could obtain four temporal images of the study area during the flood.

From the VNIR bands, the Normalized Difference Vegetation Index (NDVI) is obtained by the following equation.

$$\text{NDVI} = (\text{NIR} - \text{R}) / (\text{NIR} + \text{R}) \quad (1)$$

where NIR represents the reflectivity of band 3 and R the reflectivity of band 2. The NDVI is an index representing the degree of activity of vegetation. This value is known to be in a small value for water body, and hence the NDVI was employed to detect areas inundated by the floods. The surface temperature was obtained by converting the digital number of the TIR's band 10. Since the heat capacity of water is larger than other surface materials of the ground, the daytime surface temperature for a flooded area is lower than the normal (no flood) daytime. The extension of flooded areas were extracted by setting the thresholds for NDVI and from the change in temperature. The transition of flooded areas were then estimated by these indices from the multi-temporal ASTER images.

RESULTS OF IMAGE INTERPRETATION AND ANALYSIS

The false color composites of the multi-temporal ASTER VNIR images are shown in Figure 2. Yellow lines for the combined images of the two days indicate their boarder. In the false color composite, areas with red color show vegetation is in an active condition. In the central Thailand, there are basically three seasons: rainy season from June to October, dry-cool season from November to March, and dry-hot season form April and May. Vegetation is generally most active in rainy season, but it is still active in dry seasons due to its humid tropical climate. It is seen

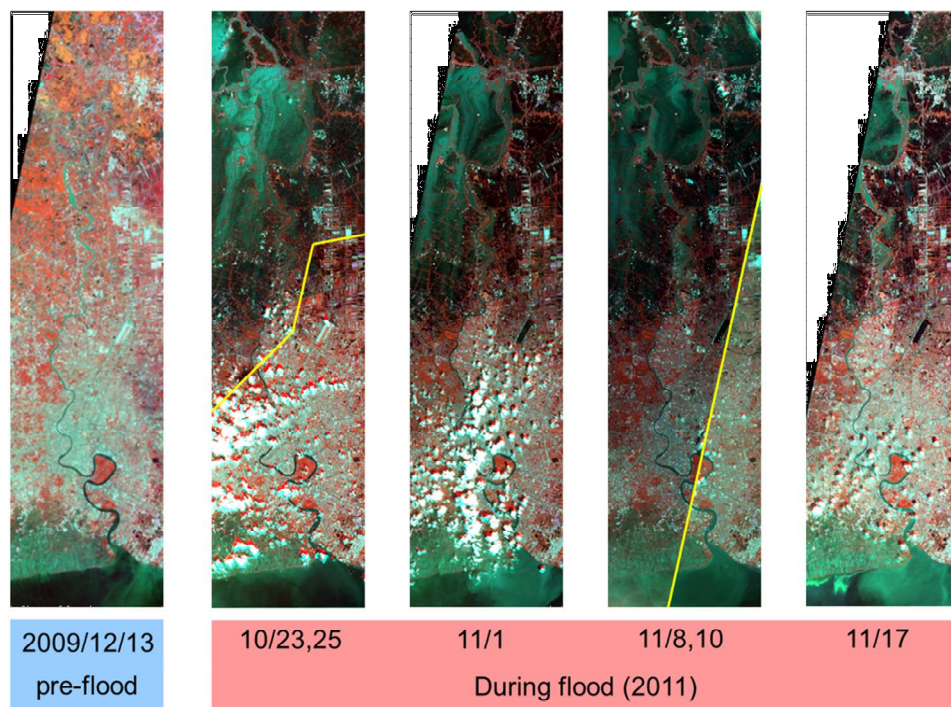


Figure 2: Multi-temporal comparison of false color composites from ASTER's VNIR bands

from the pre-event image on December 2009 that the study area is mostly covered by vegetation including rice paddy fields with some impervious land covers of urban areas, such as the central Bangkok, seen in white to light-blue color. The flooded areas can easily be recognized in the false composite as green to dark-brown color, and the flooded areas are seen to move slowly southward. In particular, it can be recognized in Don Mueang Airport's runway, which was covered by water in the images of November 2011.

Figure 3 compares the false color composite and NDVI from ASTER's VNIR images and the surface temperature from ASTER's TIR images for the pre-flood (2009/12/13) and during-flood (2011/11/17) periods. The areas of change green to dark-brown in false color, blue to violet in NDVI, and dark gray in temperature look very similar. Therefore, both the VNIR and TIR bands can be utilize to extract flooded areas. Although TIR bands have much lower spatial resolution, they can be taken even at nighttime as well as at daytime. Hence TIR images are considered to be useful to detect widely spread affected areas, especially at nighttime (Hanada and Yamazaki, 2012).

In order to determine the NDVI's threshold value for flooded areas, the cumulative distributions of of NDVI in the squared area in Figure 3 for the pre-flood (2009/12/13) and during-flood (2011/11/17) images are shown in Figure 4. In the pre-flood NDVI value, pixels below -0.4 are few but in the during-flood NDVI value, pixels in the range from -0.4 to -0.6 were increased significantly. This change is considered to be caused by the areas covered by flood water. Therefore in this study, the threshold value of NDVI for water body was determined tentatively as -0.4 although a more detailed investigation is necessary.

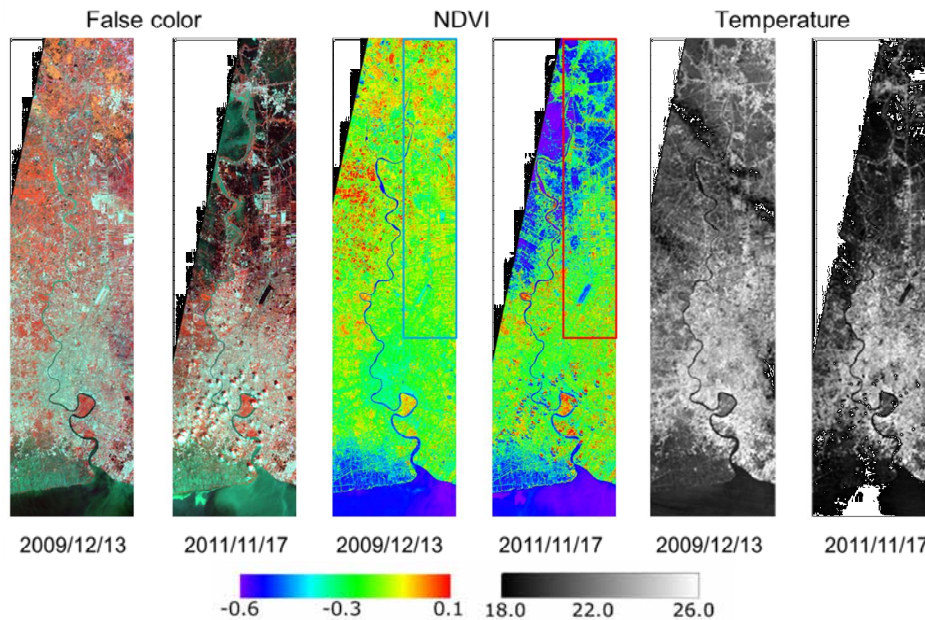


Figure 3: Comparison of false-color composite and NDVI from ASTER's VNIR images and surface temperature from ASTER's TIR images before and during the central Thailand floods

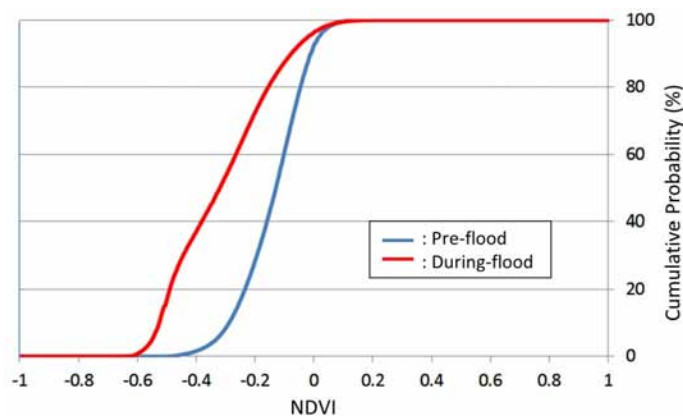


Figure 4: Comparison of cumulative distributions of NDVI in the squared area in Figure 3 for the pre-flood (2009/12/13) and during-flood (2011/11/17) images

Figure 5 shows the transition of the flooded areas estimated by applying this NDVI threshold value to the multi-temporal ASTER's VNIR images. In the figure, the pixels with the pre-event NDVI below -0.4 were excluded because these were considered as original water body. As the result, the transition of flooded areas could be extracted properly from the ASTER's VNIR images.

To observed the flood situation in more detail, three areas were extracted out of the whole study area, as shown red squares in Figure 6; they are Nava Nakorn Industrial Estate, AIT and Thammasat University's Rangsit campus, and Don Mueang Airport. Figures 7 to 9 show the close up of the false color composite, NDVI, and surface temperature from the pre- and during-flood images, and the difference of NDVI in the two images.

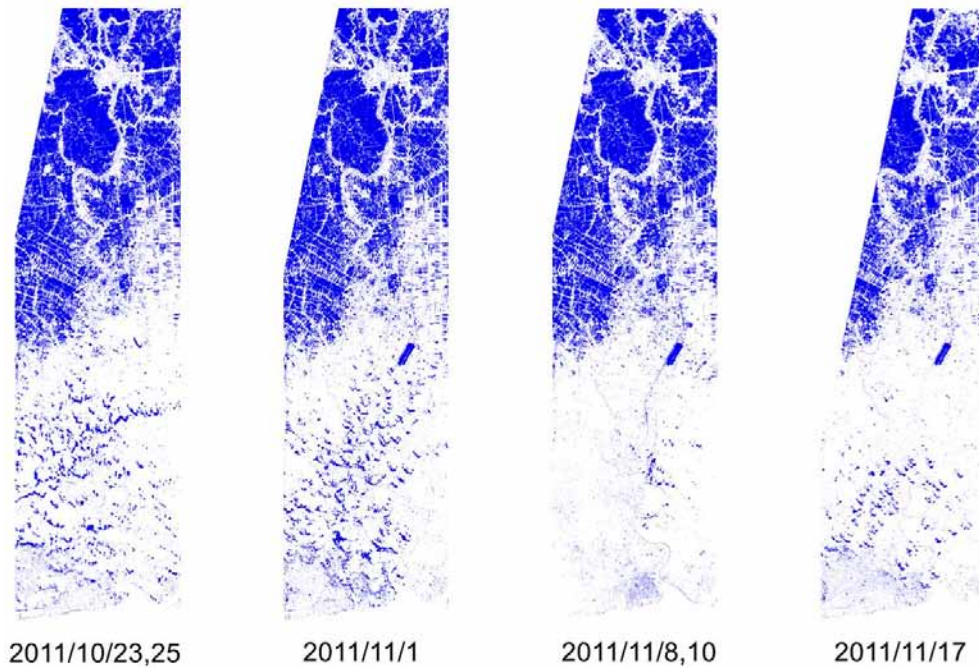


Figure 5: Multi-temporal comparison of flooded areas based on the threshold value (NDVI < -0.4)

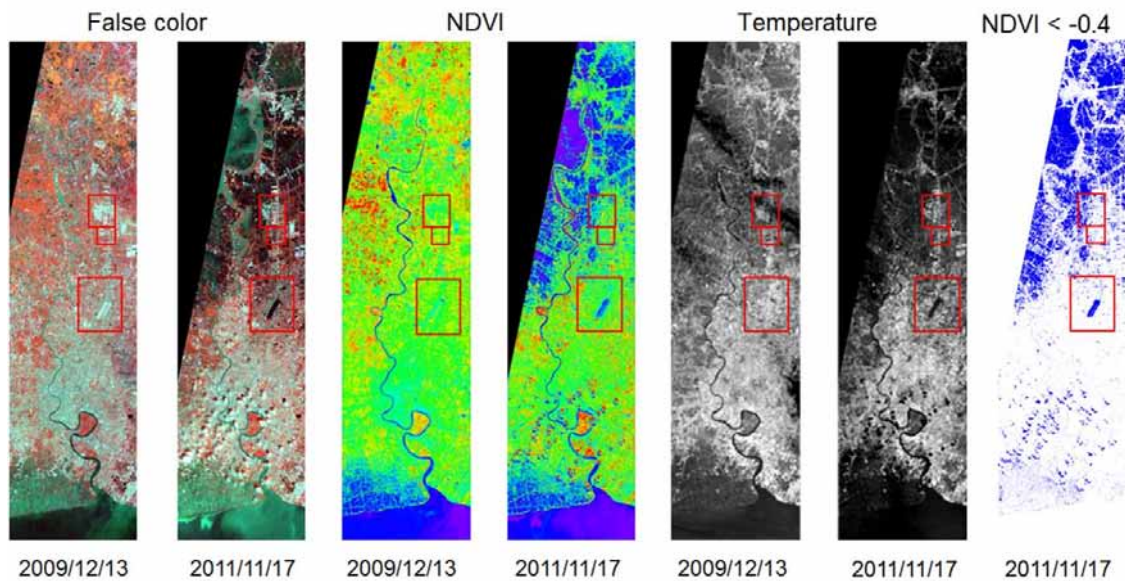


Figure 6: Location of Nava Nakorn Industrial Estate, AIT and Thammasat University's Rangsit campus, and Don Mueang Airport, from the top to bottom squares in each plot.

Nava Nakorn Industrial Estate, shown in Figure 7, was completely flooded to the level about 1.5 to 3 m above the ground surface. The flooded grounds are seen to be in dark color in the false color composite. However, the roofs of the buildings are looked unchanged because the water level was less than the roof levels. The leaves and branches of trees were also above the water level although their bottom trunks were flooded. It is noted that flood water under trees was not seen from vertical images. The comparison of NDVI values show that the NDVI values for trees in the flood period were larger than those in the non-flood period while the NDVI values for building roofs were smaller in the flood period. These differences in the same surface material due to season (vegetation) and air condition (man-made material, e.g. roof) should be considered when extracting the change in NDVI.

From the comparison of surface temperature in Figure 7, flooded areas are not so clear. This fact may be explained by several reasons: 1) mixed-pixel due to the lower resolution of TIR than VNIR images, 2) flooded water under trees was not seen from the vertical images, and 3) the average water, ground, and air temperatures were different in the two periods. Thus these elements should be taken into consideration when extracting flooded areas from TIR images.

Figure 8 shows a similar close-up of the false color composite, NDVI, and surface temperature of the pre- and during-flood images, and the difference of NDVI at the area of AIT and Thammasat University's Rangsit campus. It is known that on 17 November, 2011, this area was completely flooded. But there were many buildings and trees in the area, and thus the ground water was not so easily seen. Thus both the false color composite and NDVI gave underestimation of the flooding. There is a golf course in AIT campus at the top right of the enlarged images, and the reduction of NDVI was clearly seen there. The area extracted by the NDVI difference was not so large, suggesting the underestimation of flooded areas by this threshold value. The temperature was seen to be dropped for the flooded surface, but due to the coarse resolution of TIR, it is not so easy to extract flood water from comparison of the temperature images.

Figure 9 shows a similar close-up of the false color composite, NDVI, and surface temperature of the pre- and during-flood images, and the difference of NDVI in the area including Don Mueang Airport. Since the airport runway is a large open space and was covered by water completely, the flood situation could be detected easily from all the images: the during-flood false color composite and NDVI, the NDVI's difference, and the temperatures and its reduction. Outside of the runway, the increase of NDVI due the seasonal change was also observed in some vegetated areas.

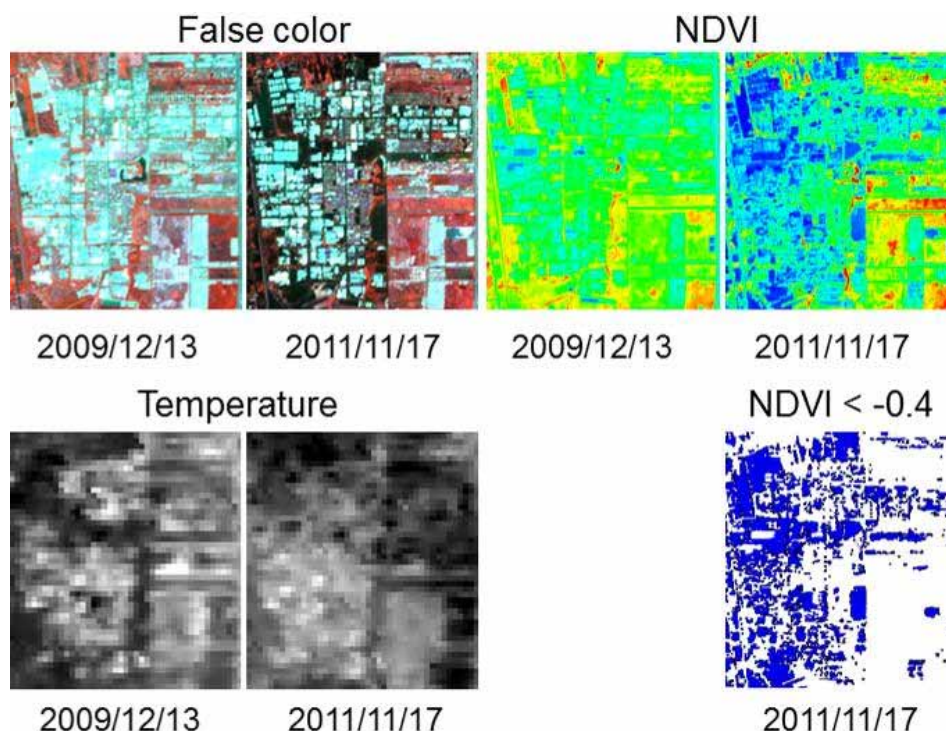


Figure 7: Close-up of the false color composite, NDVI, and surface temperature from the pre-flood and during-flood images, and the difference of NDVI at Nava Nakorn Industrial Estate

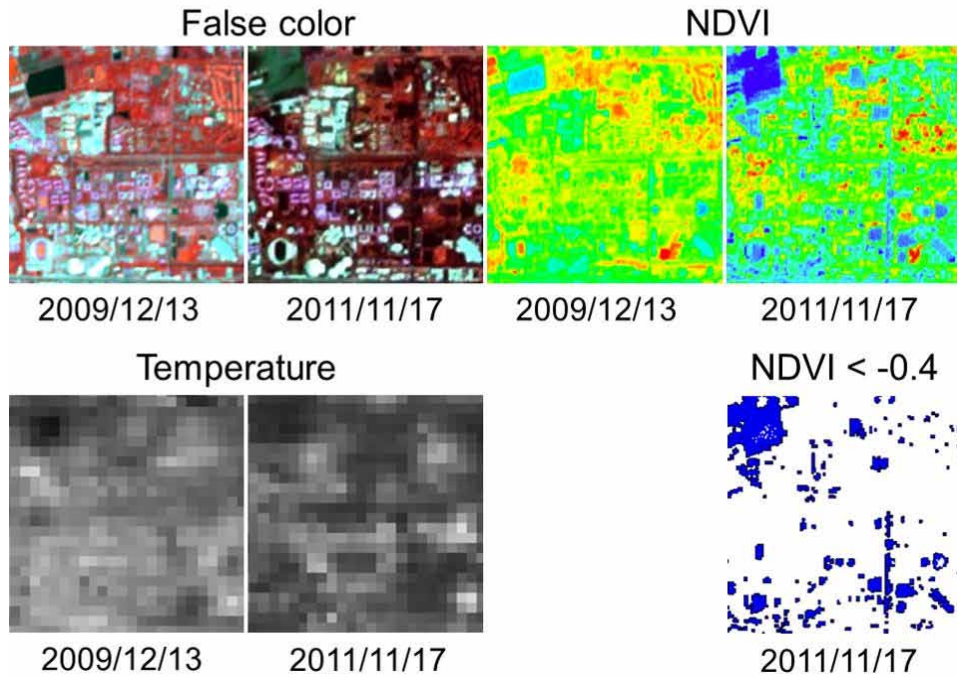


Figure 8: Close-up of the false color composite, NDVI, and surface temperature from the pre-flood and during-flood images, and the difference of NDVI at AIT and Thammasat University's Rangsit campus

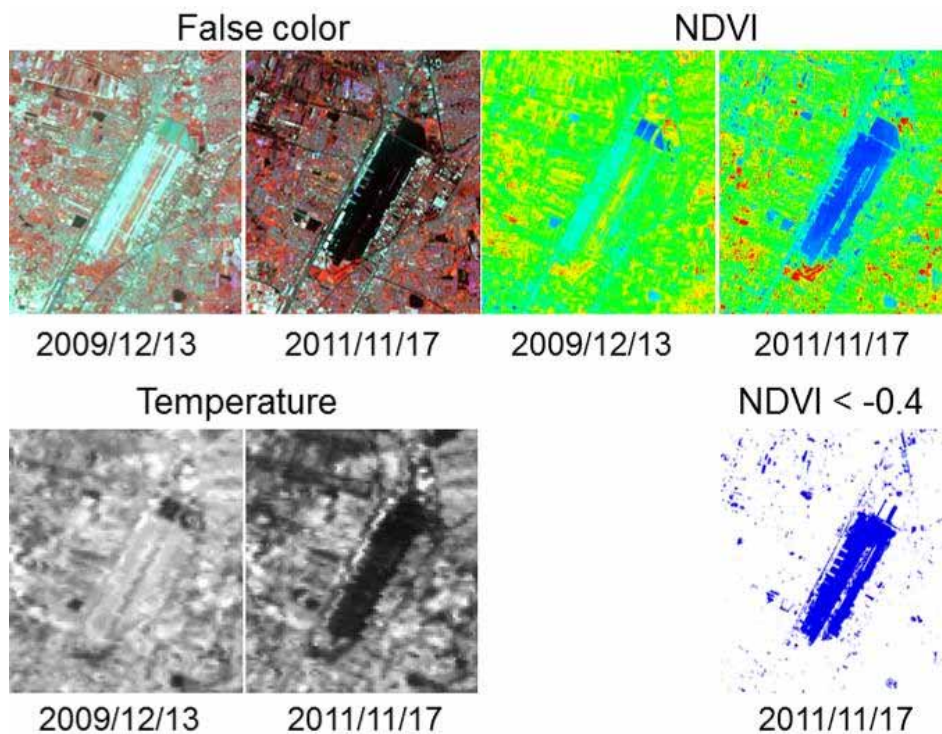


Figure 9: Close-up of the false color composite, NDVI, and surface temperature from the pre-flood and during-flood images, and the difference of NDVI at Don Mueang Airport

From these enlarged views of ASTER images, the propagation of continental floods could be easily observed from low NDVI values or the decrease in NDVI at wide open spaces with homogeneous land-cover, like university grounds and airport runways. It should be noted that the ground under trees cannot be seen and hence these observations are not valid for vertical images including many trees. The spatial resolution of images and the seasonal change in vegetation also affects the extraction capability of flooded areas from multi-temporal optical images.

CONCLUSION

In this study, the flooded areas following the 2011 central Thailand floods were extracted using ASTER's multi-temporal VNIR and TIR images. False color composite and NDVI images from VNIR and surface temperature images from TIR were produced from these ASTER data, obtained before and during the floods, to grasp the extent of the floods. The existence of water body was easily recognized for open spaces without trees and buildings from the NDVI value itself or the change in the NDVI values before and during the floods. But for densely built-up or tree-covered areas, it was difficult to observe the condition of the ground surface, and hence the omission of flood water occurred from the vertical images. The surface temperature was also be effective to detect flooding in a wide open space like airport runways although it is limited by its coarse spatial resolution. To determine the threshold values for flood extraction, however, the seasonal change in vegetation and the temperature conditions of water, air and land surface materials should be properly considered. Furthermore, the use of SAR images is considered to be most promising because SAR images can be acquired at nighttime and under cloud cover and the water surface is easily detected due to its weak backscatter.

ACKNOWLEDGMENT

ASTER images used in this study were provided by Global Earth Observation Grid (Geo Grid), National Institute of Advanced Industrial Science and Technology (AIST), Tsukuba, Japan.

REFERENCES

- Asian Institute of Technology, 2011. Inundated AIT helps Thailand map flood
URL: <http://203.159.12.32:8082/AIT/news-and-events/2011/news/inundated-ait-helps-thailand-map-flood/>
- Geo-Informatics and Space Technology Development Agency (GISTDA), 2011. Thailand Flood Monitoring System,
URL: <http://flood.gistda.or.th/>
- GHZ GEO Grid Portal, 2011. URL: <https://big.geogrid.org/gridsphere/gridsphere?cid>
- Hanada, D., and Yamazaki, F., 2012. Detection of the Flooded Area by the 2011 Tohoku Earthquake/Tsunami using ASTER Thermal Infrared Images, 9th International Conference on Urban Earthquake Engineering/ 4th Asia Conference on Earthquake Engineering, Tokyo Institute of Technology, Tokyo, Japan, CD-ROM, pp. 235-239.
- International Charter -Space and major Disaster, 2011. Flood in Thailand,
http://www.disasterscharter.org/web/charter/activation_details?p_r_p_1415474252_assetId=ACT-376
- Japan Aerospace Exploration Agency (JAXA), 2011. Results of flood monitoring in Thailand using Pi-SAR-L,
http://www.eorc.jaxa.jp/ALOS/img_up/jpi-sar_thai_nov2011_4.htm
- Japan External Trade Organization (JETRO), 2011. 2011 Thailand Floods: Current Status and Issues toward Early Flood Recovery, URL: http://www.jetro.go.jp/world/asia/th/flood/pdf/material_20111227.pdf (in Japanese).
- Kato, Y., 2007. Analysis of the Fukui Heavy Rainfall in July 2004 and the Heavy Rainfall in July 2006 by using Remote Sensing. Technology Research Bulletin, Fukui University, No. 37, pp. 335-342 (in Japanese).
- Komori, D. 2011. Preliminary Report on field survey of 2011 Chao Phraya River Flood, IMPAC-T, University of Tokyo, URL: <http://hydro.iis.u-tokyo.ac.jp/Mulabo/news/2011/ThaiFlood2011.html>
- Kouchi, K., and Yamazaki, F., 2007. Characteristics of Tsunami-Affected Areas in Moderate-Resolution Satellite Images, Transactions on Geoscience and Remote Sensing, IEEE, Vol. 45, No. 6, pp.1650-1657.
- NASA, 2012. ASTER: Advanced Spaceborne Thermal Emission and Reflection Radiometer.
URL: <http://asterweb.jpl.nasa.gov/>
- Yamazaki, F., Matsuoka, M., Warnitchai, P., Polngam, S., Ghosh, S., 2005. Tsunami Reconnaissance Survey in Thailand Using Satellite Images and GPS, Asian Journal of Geoinformatics, Vol. 5, No. 2, pp. 53-61.
- Yamazaki, F., 2012. Survey Report of 2011 Thailand Flood, Yobojiho, The General Insurance Association of Japan, No. 248, pp. 37-38 (in Japanese).
- Ziegler, A. D., Lim, H. S., Tantasarin, C., Jachowski, N. R., Wasson, R., 2012. Floods, false hope, and the future. Hydrol. Process. Published online in Wiley Online Library (wileyonlinelibrary.com). DOI: 10.1002/hyp.9260